Laser spectroscopy of LaS: Hyperfine structure in the $B\,^2\Sigma^+ - X\,^2\Sigma^+$ (0,0) band

S. G. He, W. S. Tam, J. W-H. Leung, and A. S-C. Cheung[a)]
Department of Chemistry, The University of Hong Kong, Pokfulam Road, Hong Kong

(Received 26 April 2002; accepted 31 May 2002)

The (0,0) band of the $B\,^2\Sigma^+ - X\,^2\Sigma^+$ transition of LaS near 726 nm has been studied at high resolution using laser vaporization/reaction supersonic free jet expansion and laser induced fluorescence spectroscopy. Spectra taken at a resolution of about 50 MHz show resolved hyperfine structure which is caused principally by the unpaired $6s\sigma$ electron in the ground state interacting with large magnetic moment of the $^{139}_{57}$La nucleus with nuclear spin $I=7/2$. The $X\,^2\Sigma^+$ state of LaS is in good Hund's case ($b_{\beta s}$) coupling, however, the upper state, $B\,^2\Sigma^+$, is close to case ($b_{\beta J}$) coupling. A total of 1850 rotational-hyperfine transition lines have been assigned and measured. Accurate rotational, spin and hyperfine parameters for the $B\,^2\Sigma^+$ and $X\,^2\Sigma^+$ states have been obtained, which give information about the electron distribution in the molecule. © *2002 American Institute of Physics.* [DOI: 10.1063/1.1495405]

I. INTRODUCTION

Diatomic transition metal sulfides are molecules of astrophysical interest. Amongst these sulfides, TiS (Refs. 1, 2) and ZrS (Refs. 3, 4) have been identified in S-type Mira variable stars. Despite this importance, a recent review article by Harrison[5] shows that the diatomic transition metal sulfides could still be ranked among the least studied diatomic transition metal systems. Our laboratory has been performing high resolution laser spectroscopic studies on these sulfides which include TiS,[6,7] VS,[8,9] and CrS.[10,11] It is hoped that the data we offer could encourage astronomers to search for the presence of more transition metal sulfides in the atmosphere of cool stars. Lanthanum sulfide (LaS) is obviously one of the molecules that falls into this category.[12] The spectrum of LaS was first studied by Marcano and Barrow,[13] the $B\,^2\Sigma^+ - X\,^2\Sigma^+$ transition was photographed and partial rotational analysis was performed. Winkel *et al.*[14] recorded the Fourier transform (FT) spectrum of LaS in the region 1800–16000 cm^{-1}, and reported the vibrational analysis of both the $A\,^2\Pi - X\,^2\Sigma^+$ and the $B\,^2\Sigma^+ - X\,^2\Sigma^+$ systems. Recently, Andersson *et al.*[15] obtained higher resolution FT spectrum and performed rotational analysis of both the $A\,^2\Pi - X\,^2\Sigma^+$, $B\,^2\Sigma^+ - X\,^2\Sigma^+$ and a new $A\,^2\Pi - A'\,^2\Delta$ transition, and reported vibrational and rotational constants for $X\,^2\Sigma^+$, $B\,^2\Sigma^+$, $A\,^2\Pi$, and $A'\,^2\Delta$ states. However, detailed analysis of the hyperfine structure of the $B\,^2\Sigma^+ - X\,^2\Sigma^+$ transition has never been performed.

The large magnetic hyperfine structure in the LaS molecule is caused by the interaction of the unpaired $6s\sigma$ electron with the magnetic moment of the $^{139}_{57}$La. This magnetic hyperfine structure gives useful information about the bonding in the molecule because hyperfine parameters are related to expectation values of the coordinates of the electron near the spinning nuclei.[16–18] The Frosch and Foley parameters[16] determined experimentally for a $^2\Sigma^+$ provide information on the probability density of finding the electron at the nucleus, $\langle \psi^2(0) \rangle$, and the angular dependence of atomic wave function averaged over the electronic space coordinates, $\langle (3\cos^2\theta_i - 1)/r^3 \rangle_{av}$.

In this paper, we report the study of the $B\,^2\Sigma^+ - X\,^2\Sigma^+$ (0,0) band of LaS using the technique of laser vaporization/reaction supersonic free jet expansion and laser induced fluorescence spectroscopy. The magnetic hyperfine structure caused by the $^{139}_{57}$La nucleus ($I=7/2$) is well resolved. Least-squares fit of the hyperfine transition line positions yielded a comprehensive set of rotational, spin, and hyperfine parameters for both the $B\,^2\Sigma^+$ and $X\,^2\Sigma^+$ states. The magnetic hyperfine parameters obtained are interpreted, which yielded information about the occupation of molecular orbitals giving rise to the states studied in this molecule.

II. EXPERIMENTAL DETAIL

A laser vaporization/reaction supersonic free jet-laser induced fluorescence (LIF) experimental apparatus similar to the one used in this experiment has been discussed in our earlier publications.[6,19] The only different between the earlier version and this one is the use of a vacuum system that consists of a source chamber and a detection chamber separated by a 3 mm diam skimmer. Each chamber was pumped by a 600 l/s turbo molecular pump. A laser pulse of 532 nm and 10 mJ from a Nd:YAG laser was synchronized and appropriately delayed, and focused onto a lanthanum metal rod to produce metal vapor. LaS was produced, in the source chamber, by reacting laser ablated La atoms from the lanthanum rod with a mixture of 4% CS_2 in argon released by a pulsed valve. A molecular beam of LaS was obtained in the detection chamber by skimming the output from the supersonic laser ablation/reaction source. The pulsed valve–Nd:YAG system was operated at a repetition rate of 10 Hz and the backing pressure of the pulsed valve was 5.5 atm. The background pressures measured in the source and detec-

a)Author to whom correspondence should be addressed. Electronic mail: hrsccsc@hku.hk; Fax: (852) 2857 1586; Tel.: (852) 2859 2155.

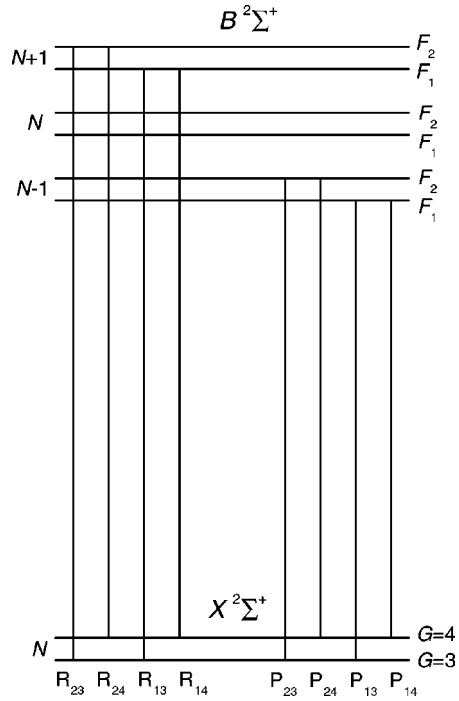

FIG. 1. Labeling of the branches in the $B\,^2\Sigma^+ - X^2\Sigma^+$ transition of LaS.

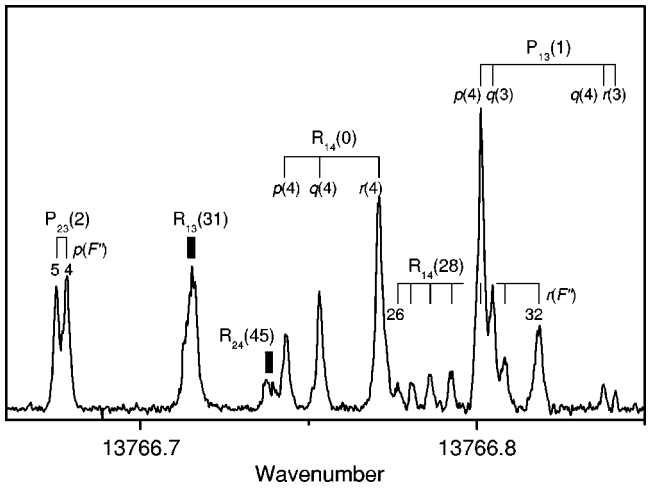

FIG. 2. High resolution spectrum of the $R_{14}(0)$ and $P_{13}(1)$ lines of the $B\,^2\Sigma^+ - X^2\Sigma^+$ band of LaS at 13 766 cm^{-1} showing the resolved hyperfine components.

tion chambers were about 4×10^{-5} and 2×10^{-6} Torr, respectively, when the system was in operation.

LaS molecules were excited by laser radiation, at right angles to the expansion axis about 5 cm downstream from the skimmer, from a tunable Ti:sapphire ring laser pumped by an argon ion laser. Laser induced fluorescence signals were collected at right angles to the plane made by the expansion and excitation axes by means of a lens system and detected by a Hamamatsu R636-10 super red photomultiplier tube. The signals were pre-amplified before feeding into a fast digital oscilloscope for averaging. Since these signals were recorded using a signal-averaging technique, we had examined the effect of various scanning speeds and eventually settled at a rate of 0.2 cm^{-1}/8 min scan. The width of the molecular transition lines of LaS was measured to be about 45–50 MHz, depending on the backing pressure at the pulsed valve and the background pressure in the detection chamber. The wavelength of the Ti:sapphire laser output was measured by a wave meter at a rate of 1 Hz and an accuracy of 1 part in 10^7. The absolute accuracy of the wave meter is about ±0.001 cm^{-1}, which was calibrated using iodine lines.[20] Hundreds of scans were made and connected together by a computer program using the wavemeter readings.

III. RESULTS AND DISCUSSION

A. Hyperfine structure in the $B\,^2\Sigma^+$ and $X\,^2\Sigma^+$ states

The (0,0) band of the $B\,^2\Sigma^+ - X\,^2\Sigma^+$ transition of LaS has been recorded with a resolution of about 50 MHz (0.0017 cm^{-1}). The main features of the LIF spectrum are the four heads at 13 770.3, 13 769.8, 13 768.4, and 13 767.9 cm^{-1} corresponding to the heads of the four R_{23}, R_{24}, R_{13}, and R_{14} branches, respectively. Due to hyperfine and spin splitting in the $X\,^2\Sigma^+$ and the $B\,^2\Sigma^+$ states, this band consists of 8 branches, which are labeled according to the structure displayed in Fig. 1. A separation of 0.47 cm^{-1} between the heads of R_{23} and R_{24}, and also R_{13} and R_{14} is easily noticed in the recorded spectrum, which arises from the hyperfine splitting in the $X\,^2\Sigma^+$ state that conforms to the case ($b_{\beta s}$) coupling[17] with large Fermi contact interaction.

In a pure Hund's case (b) coupling scheme of a $^2\Sigma^+$ state, the electron spin **S** is not coupled to any vector and precess freely; practically there will always be a small spin-rotation interaction, described by the operator $\gamma\,\mathbf{N}\cdot\mathbf{S}$. When a nucleus with nonzero **I** is present, there will be magnetic hyperfine interaction between the nuclear and electron spins. The resulting energy level pattern depends on which of these two interactions is the larger. When the unpaired electron is in a molecular orbital which is essentially formed from an s atomic orbital, the Fermi contact interaction, $b_F\,\mathbf{I}\cdot\mathbf{S}$, couples the **S** to **I** more strongly than the spin-rotation interaction couples **S** to **N**, the coupling scheme is case ($b_{\beta s}$) with

$$\mathbf{S}+\mathbf{I}=\mathbf{G};\quad \mathbf{N}+\mathbf{G}=\mathbf{F}. \tag{1}$$

The intermediate quantum number G is that for the total spin, which is electron spin plus nuclear spin.[17] The $X\,^2\Sigma^+$ state of LaS is in case ($b_{\beta s}$) coupling. $^{139}_{57}$La has a spin $I=7/2$, which means that the rotational levels of the $X\,^2\Sigma^+$ are split into $G=3$ and $G=4$ groups. Each group consists of, at the most, $2G+1$ hyperfine components. The observed splitting between the $G=3$ and $G=4$ groups is about 0.47 cm^{-1}, which implies the Fermi contact parameter in $X^2\Sigma^+$ state of LaS is quite large. The $X\,^2\Sigma^+$ state of LuO (Refs. 21, 22) and CoC (Refs. 23, 24) is also in case ($b_{\beta s}$) coupling with a large G group splitting. The fully developed hyperfine manifold in case ($b_{\beta s}$) with $G=3$ and $G=4$ components are, respectively, with 7 and 9 hyperfine components.

In the case of the hyperfine interaction is small when compare to the spin-rotation coupling, a reasonable choice of basis set is given by the case ($b_{\beta J}$) coupling scheme,

$$\mathbf{N}+\mathbf{S}=\mathbf{J};\quad \mathbf{J}+\mathbf{I}=\mathbf{F}. \tag{2}$$

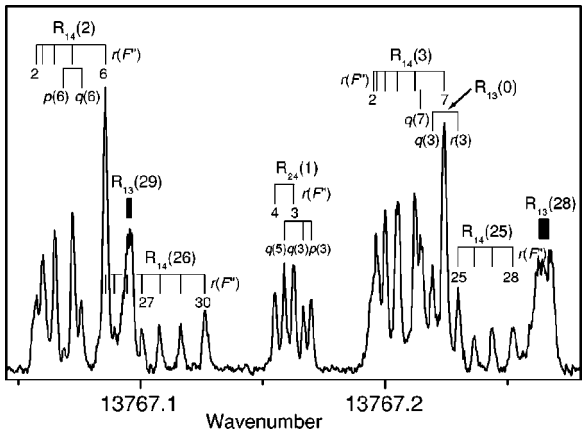

FIG. 3. High resolution spectrum of the $R_{13}(0)$ and $P_{24}(1)$ lines of the $B\,^2\Sigma^+$–$X\,^2\Sigma^+$ band of LaS at 13 767 cm^{-1} showing the resolved hyperfine components.

The excited $B\,^2\Sigma^+$ state conforms to this coupling scheme, because the $B\,^2\Sigma^+$ has large spin-rotation interaction but very small magnetic hyperfine interaction. The spin rotation interaction gives rise to spin splitting of $F_1$and F_2 groups for the $^2\Sigma^+$ state. However, in case $(b_{\beta J})$ coupling, both of the F_1 and F_2 groups gives at the most $2I+1$ hyperfine components. In LaS, since $I=7/2$ the hyperfine components for each F group are 8.

Figures 2 and 3 show the first lines of the R and P branches. The $\Delta F=-1$, 0, and $+1$ transitions are respectively labeled with $p(F)$, $q(F)$, and $r(F)$. Using these labels, the $R_{14}(0)$ transition has the $p(4)$, $q(4)$, and $r(4)$ hyperfine lines. Similarly for $P_{13}(1)$ and $R_{14}(1)$ lines, the hyperfine lines are clearly resolved and assigned. The hyperfine energy levels for the ground state are given in Fig. 4. Even though the spin splitting is large (0.47 cm^{-1}), the ground state spin-rotation constant, γ, is quite small ($-0.000\,775\,3$ cm^{-1}). The hyperfine level pattern of the $G=3$ and 4 groups basically depends on the size of the γ parameter. The folding back of the smallest F component of the $G=3$ and 4 groups at lower rotational quantum number N is due primarily to the fact that γ is small and negative. Since the spin-rotation interaction is N dependent, the spin angular momentum of the $X\,^2\Sigma^+$ state is progressively uncoupled from the nuclear spin under high rotation to become case $(b_{\beta J})$ coupling. For LaS, we notice that the spin uncoupling processes proceed very slowly, it is far from being completed even at the highest N values observed. Figure 5 shows the energy level pattern for the excited $B\,^2\Sigma^+$ state. Because of no sizable Fermi contact interaction, the $B\,^2\Sigma^+$ rotational levels are essentially split into the F_1 and F_2 spin components. The separation between F_1 and F_2 components is N dependent. The hyperfine level pattern of F_1 and F_2 group of levels depends on mainly the size of the upper state b and c parameter. The spin-rotation constant of the upper state is 0.096 479 8 cm^{-1}, which is about 124 times larger than the ground state. It is important to note the spread of the hyperfine energy levels and the ordering of the hyperfine components in the G groups in case $(b_{\beta s})$ and the F groups in case $(b_{\beta J})$. At relatively large N values, the $G=3$ and 4 groups have a spread of energy about 0.2 cm^{-1}; the $G=3$ group has the highest F component with the highest

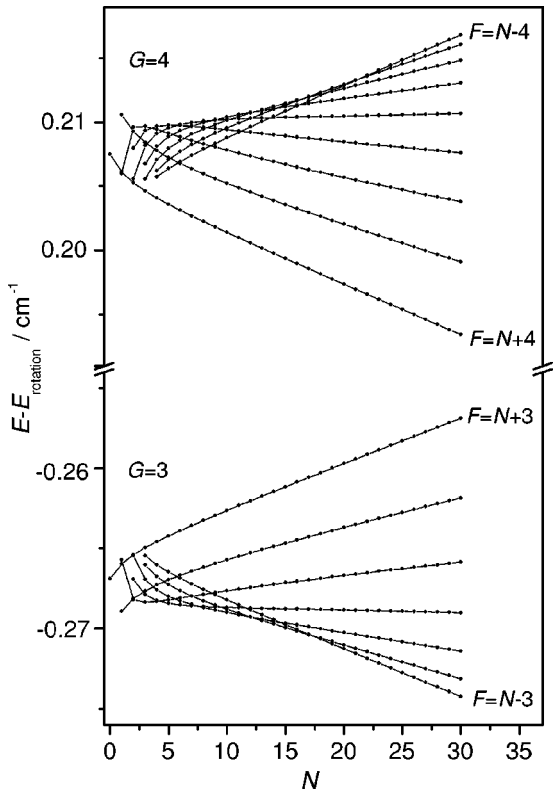

FIG. 4. Hyperfine energy levels of the $X\,^2\Sigma^+$ state, $v=0$ level of LaS plotted against the rotational quantum number N showing the uncoupling from case $(b_{\beta s})$ toward case $(b_{\beta J})$. Levels are calculated from the molecular constants given in Table II.

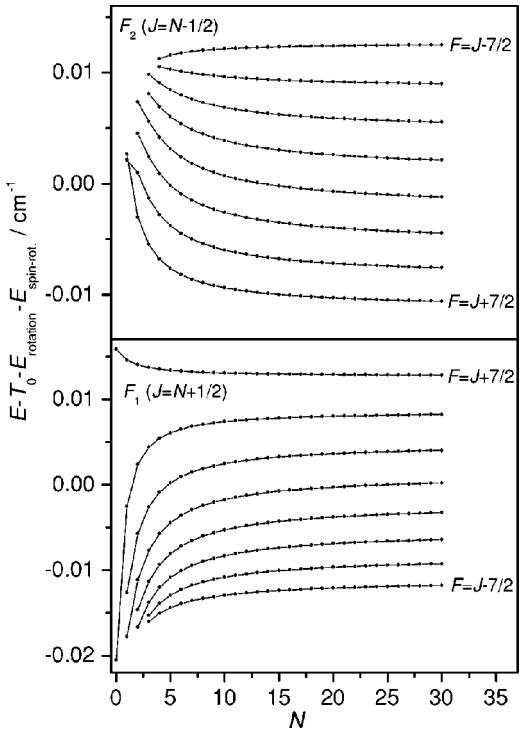

FIG. 5. Hyperfine energy levels of the $B\,^2\Sigma^+$ state, $v=0$ level of LaS plotted against the rotational quantum number N in case $(b_{\beta J})$ coupling. Levels are calculated from the molecular constants given in Table II.

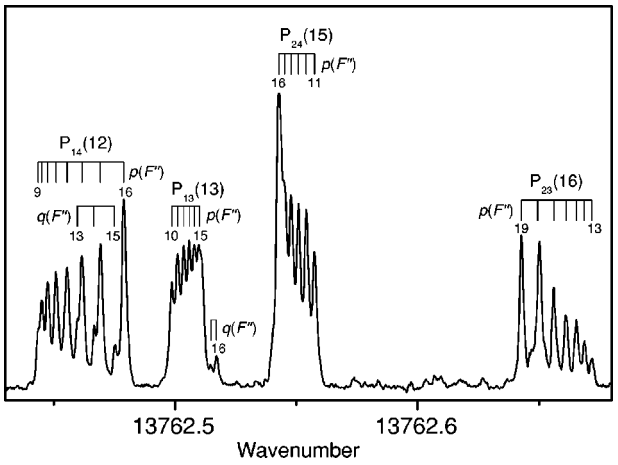

FIG. 6. High resolution spectrum of the P_{13}, P_{14}, P_{23}, and P_{24} branches of the $B\,^2\Sigma^+$–$X\,^2\Sigma^+$ band of LaS showing resolved hyperfine components.

energy, but the $G=4$ group is reversed the highest F component with the lowest energy. Such pattern can be found in the upper state even at low N values, where F_1 is similar to $G=3$ and F_2 is similar to $G=4$. This situation gives rise to wider hyperfine width in the transition lines of the P_{14}, R_{14}, P_{23}, and R_{23} branches and narrower hyperfine width of the P_{13}, R_{13}, P_{24}, and R_{24} branches. Figure 6 displays the four P branches of LaS showing that the wider lines belong to the P_{14} and P_{23} and the narrower lines are for the P_{13} and P_{24} branches. Even though the $B\,^2\Sigma^+$–$X\,^2\Sigma^+$ (0,0) band was rotationally analyzed by Andersson *et al.*,[15] the FT spectrum was recorded at 2500 K and essentially only higher N lines were identified. Under our experimental conditions, LaS molecules produced were cold and only relatively low N lines were recorded in our spectrum.

B. Determination of spectroscopic parameters

The effective molecular Hamiltonian for a $^2\Sigma^+$ state with hyperfine interaction is given by

$$\mathbf{H}=B\mathbf{N}^2-D\mathbf{N}^4+\gamma\mathbf{N}\cdot\mathbf{S}+b\mathbf{I}\cdot\mathbf{S}+cI_zS_z + eT^2(\mathbf{Q})\cdot T^2(\nabla E), \quad (3)$$

where B and D are the rotational constant and its centrifugal distortion, γ is the spin-rotation constant, b is the Fermi contact parameter, and c is the dipolar interaction, and the last term is the nuclear electric quadrupole coupling. The magnetic hyperfine terms have been taken according to Frosch and Foley's definition,[16] where the true Fermi contact parameter, b_F, is given by $b_F=b+c/3$. The Hamiltonian matrix elements in the case ($b_{\beta S}$) coupling scheme expressed in tensor and algebraic forms are given in Barnes *et al.*,[23] which include diagonal and off-diagonal elements in quantum number N and G. A computer program was written using the Fortran language to construct the Hamiltonian matrix from these matrix elements to calculate hyperfine energy levels for both the $X\,^2\Sigma^+$ and $B\,^2\Sigma^+$ states. An additional subroutine was written and used to identify the F_1 and F_2 labeling of the $B\,^2\Sigma^+$ state in the case ($b_{\beta J}$) coupling.

A total of 1850 transition lines was identified and measured, a list of the wave numbers of the $B\,^2\Sigma^+$–$X\,^2\Sigma^+$ (0,0) band of LaS measured in this work is available from EPAPS.[25] Table I summarizes hyperfine transition lines of all the eight branches that were used in the least squares fit. Due to heavy overlap and the nature of the hyperfine transitions described earlier, only a few lines of the R_{13} branch were resolved even at our resolution. A data set consisting of 1140 resolved hyperfine lines were fitted simultaneously. In the initial stage only the higher N lines were included, but in the end the whole data set with N up to 39 were used. Rotational constants reported by Andersson *et al.*[15] were found to be useful as initial constants to assist our least squares fit. The final molecular constants and those from earlier work[15] are both listed in Table II. The rotational and hyperfine constants for both the $B\,^2\Sigma^+$ and the $X\,^2\Sigma^+$ states are well determined. The weighted root-mean-squares error (RMS) of our final fit was 0.000 79 cm^{-1}. For the rotational centrifugal distortion constants D, our fitted values are larger than those of Andersson *et al.*[15] With the same data set, we have tried to restrict the D constant to the value of Andersson *et al.*[15] for the $X\,^2\Sigma^+$ state but the RMS error jumped up to over 0.0011 cm^{-1} and the e^2Qq_o parameter was found to be undetermined. We also noticed that the B values of both the ground and excited states are slightly higher than those of Andersson *et al.*[15] Our data set consists of mainly low N lines, which is definitely more comfortable with the slightly larger values of D constants in both states.

C. Interpretation of hyperfine parameters

The large size of the Fermi contact parameters for the ground state reflects the occupation of the $s\sigma$ molecular orbital, which is appropriate and consistent that the $X\,^2\Sigma^+$ state

TABLE I. Summary of hyperfine transition lines used in the least squares fit.

	No. of lines with $\Delta F=\Delta N$	No. of lines with $\Delta F\neq\Delta N$	Ground state lowest N	Ground state highest N	Unweighted-RMS (cm^{-1})	Weighted-RMS (cm^{-1})
R_{24}	103	4	0	18	0.000 69	0.000 62
R_{23}	127	15	4	30	0.000 56	0.000 51
R_{14}	174	10	0	39	0.000 80	0.000 79
R_{13}	53	1	0	22	0.000 81	0.000 72
P_{24}	127	0	2	21	0.000 82	0.000 81
P_{23}	201	8	2	37	0.000 88	0.000 88
P_{14}	173	35	1	31	0.000 92	0.000 90
P_{13}	83	26	1	23	0.000 82	0.000 80
Total	1140				0.000 81	0.000 79

TABLE II. Rotational and hyperfine constants for the $v=0$ level of the $B\,^2\Sigma^+$ and $X\,^2\Sigma^+$ states of LaS (in cm^{-1}).[a]

	$X\,^2\Sigma^+$		$B\,^2\Sigma^+$	
	This work	Ref. 15	This work	Ref. 15
T_0	0	0	13 766.789 34(42)	13 766.786 51
B	0.117 015 5(14)	0.116 976	0.111 073 5(14)	0.111 032
10^7 D	0.511(11)	0.307 7	0.543(10)	0.326 3
γ	−0.000 775 3(60)		−0.096 479 8(38)	−0.096 455
b	0.117 026(37)	0.117 97	0.006 816(30)	
c	0.004 762(93)		0.006 84(21)	
e^2Qq_0	−0.001 11(69)		−0.005 85(67)	

[a]Values given in parentheses are one standard error in least significant figures quoted.

arises from the electronic configuration $(8\pi)^4(17\sigma)^1$. The 17σ orbital is mainly of the character of the $6s\sigma$.[15] The true b_F parameter can be calculated from the measured b and c constants,

$$b_F = b + c/3 = 0.118\,613 \ \text{cm}^{-1}. \tag{4}$$

It is evident that the hyperfine parameters[16] are extremely sensitive to the nature of the electronic state and provide a direct measure of the quality of available *ab initio* calculations. A common method of interpreting these parameters is to use a free atom comparison method to compare the determined parameters with *ab initio* results from atoms.[26] Strictly speaking, the b_F parameter has contributions from all unpaired electrons, which is indicated by the summation in the following expression:[27]

$$b_F = \left(\frac{\mu_0}{4\pi hc}\right)\frac{8\pi}{3} g g_N \mu_B \mu_N \left(\frac{1}{2S}\right)\sum_i \langle \psi_i^2(0)\rangle. \tag{5}$$

However, the dominant contribution to the b_F parameter is from the $6s\sigma$ electron with an expectation value $\langle \psi^2(0)\rangle_{6s}$. The nuclear magnetic moment of La is 2.7832 nuclear magneton[28] and the expectation value $\langle \psi^2(0)\rangle_{6s}$ from *ab initio* calculation[29] is 5.492 a.u.$^{-3}$,

$$b_F = 0.003\,186\,25 \times \frac{8\pi}{3} \times \frac{2.7832}{7/2} \times 5.492$$
$$= 0.116\,56 \ \text{cm}^{-1}. \tag{6}$$

This value is in excellent agreement with our experimental determination, which indicates the hyperfine interaction in the $X\,^2\Sigma^+$ state is dominated by contribution from the La atom. The $B\,^2\Sigma^+$ state arises from the electronic configuration $(8\pi)^4(18\sigma)^1$, where the 18σ orbital is an antibonding orbital formed mainly from the $5d\sigma$ orbital of the lanthanum atom and the $3p\sigma$ orbital of the sulfur atom. The value of the b_F parameter of the $B\,^2\Sigma^+$ state should be zero if there is no $s\sigma$ character in the 18σ orbital. The small value of b_F could come from spin polarization of the 18σ antibonding electron parallel to the spin of the unpaired lanthanum electron in the region near the La nucleus.[27]

As discussed by Frosch and Foley,[16] the magnetic hyperfine dipolar constant c and electric quadrupole parameter e^2Qq_0 can be compared in similar fashion to the atomic values. Using their expressions,[27]

$$c = \left(\frac{\mu_o}{4\pi hc}\right)\frac{3}{2} g g_N \mu_B \mu_N \left(\frac{1}{2S}\right)\sum_i \langle 3\cos^2\vartheta_i - 1\rangle\langle r_i^{-3}\rangle, \tag{7}$$

and

$$\langle e^2Qq_o\rangle = -\left(\frac{e^2Q}{4\pi\varepsilon hc}\right)\sum_i \langle 3\cos^2\vartheta_i - 1\rangle\langle r_i^{-3}\rangle. \tag{8}$$

For the magnetic hyperfine dipolar term in Eq. (7), the summation is over only the unpaired electrons, while for the electric quadrupole term in Eq. (8), all valence electrons are included. Since the 17σ orbital can be written as

$$|17\sigma\rangle = C_{6s}|\text{La}6s\sigma\rangle + C_{5d}|\text{La}5d\sigma\rangle + C_{3p}|S3p\sigma\rangle, \tag{9}$$

the C_{6s} coefficient is the largest coefficient in the expression and the C_{5d} and C_{3p} coefficients are much smaller. For the $X\,^2\Sigma^+$ state, since the unpaired electron occupies the $s\sigma$ orbital, the angular dependence $\langle 3\cos^2\theta - 1\rangle_{s\sigma}$ for both c and e^2Qq_o is zero.[27] The theoretical value for the c and e^2Qq_o parameters should be zero, however, the small nonzero value of these two parameters may arise from the polarization of the core and also with contribution from an electronic configuration that contains unpaired $5d\sigma$ electron.[23]

The 18σ orbital consists of the same atomic orbitals as in Eq. (9), but the C_{5d} coefficient is the largest. For the $B\,^2\Sigma^+$ state, the angular dependence, $\langle 3\cos^2\theta - 1\rangle_{d\sigma}$, for the $d\sigma$ electron is $(\frac{4}{7})$.[27] The radial expectation value $\langle r^{-3}\rangle_{5d}$ for the $5d$ electron is tabulated in Morton and Preston.[29] With the value of the nuclear quadruple moment of the La atom is 0.22×10^{-30} m^2, we obtain theoretical value for c and e^2Qq_o for the $B\,^2\Sigma^+$ state as follows:

$$c = 0.003\,186\,25 \times \frac{3}{2} \times \left(\frac{2.7832}{7/2}\right) \times \left(\frac{4}{7}\right) \times 3.127$$
$$= 0.006\,79 \ \text{cm}^{-1}, \tag{10}$$

$$\langle e^2Qq_o\rangle = -0.007\,837\,6 \times 0.22 \times \left(\frac{4}{7}\right) \times 3.127$$
$$= -0.003\,08 \ \text{cm}^{-1}. \tag{11}$$

The agreement between the theoretical and the experimental dipolar constant c for the $B\,^2\Sigma^+$ state is excellent, which is consistent with the expectation that the 18σ orbital is dominated by contribution from $5d\sigma$ orbital of the La

atom. However, the agreement of the electric quadruple parameter is not as good. It should be noted that the electric quadruple parameter has contributions from valence electrons of the nucleus in the molecule, charge distributions associated with adjacent atoms, and the distortion of the closed shell electrons around the nucleus, which makes this parameter difficult to interpret. Since our calculation only includes contribution from the unpaired electron to the $\langle e^2Qq_o\rangle$ parameter, the agreement could still be considered as reasonable. Even though our method of interpreting these parameters using a free atom comparison approach is successful, we would like to point out that this approach is not always valid, as demonstrated in the analysis of the ESR results for SiO^+,[30] and the electronic spectrum of CoC.[23]

LaS has a valence electronic configuration similar to that in LaO and the hyperfine interaction in LaO is also dominated by the La atom, it would be instructive to compare the determined hyperfine parameters for these two molecules. The following is a comparison of these parameters for the $X\,^2\Sigma^+$ and the $B\,^2\Sigma^+$ states of LaS and LaO (cm^{-1}):

	$X\,^2\Sigma^+$ state		$B\,^2\Sigma^+$ state	
Parameter	LaO[31]	LaS	LaO[32]	LaS
b	0.11831	0.11703	0.01954	0.00682
c	0.00314	0.00476	0.00664	0.00684
b_F	0.11935	0.11861	0.02175	0.00903
e^2Qq_o	−0.00283	−0.00111	−0.00645	−0.00585

The agreement of these parameters for the $X\,^2\Sigma^+$ and the $B\,^2\Sigma^+$ states of these two molecules is reasonably good except the b values for the $B\,^2\Sigma^+$ state. The b value alone is difficult to interpret, however, the b_F value is a direct measure of the contribution of the expectation value $\langle\psi^2(0)\rangle_{6s}$. For the $B\,^2\Sigma^+$ state, the difference in b_F values of LaS and LaO could be understood as the contribution of the $6s$ orbital to the molecular orbital in these two molecules is different. We are confident to conclude that the hyperfine interaction in both molecules is dominated by contributions from the La nucleus. If *ab initio* calculation results detailing the contributions of various atomic orbitals in forming the molecular orbitals giving rise to $X\,^2\Sigma^+$ and the $B\,^2\Sigma^+$ states of both LaS and LaO molecules are available, it is expected that the minor differences in these parameters could be rationalized easily.

IV. SUMMARY

This work reports high-resolution laser spectroscopic study of the $B\,^2\Sigma^+$–$X\,^2\Sigma^+$ (0,0) band of LaS and the analysis yielded a full set of hyperfine parameters for both the $B\,^2\Sigma^+$ and the $X\,^2\Sigma^+$ states. Because of the difference in size of the constants b and γ for the two $^2\Sigma^+$ states, the $B\,^2\Sigma^+$ and $X\,^2\Sigma^+$ states are conformed to case ($b_{\beta J}$) and ($b_{\beta s}$) couplings, respectively. A comparison of the experimentally determined hyperfine parameters of the $X\,^2\Sigma^+$ and the $B\,^2\Sigma^+$ states with the theoretical value derived from an *ab initio* wave function give a quantitative description of the nature of the molecular orbitals.

ACKNOWLEDGMENTS

A.S.C.C. thanks Professor S. P. Davis for sending us a list of the rotational transition lines of the $B\,^2\Sigma^+$–$X\,^2\Sigma^+$(0,0) band. The work described here was supported by a grant from the Committee on Research and Conference Grants of the University of Hong Kong. We thank Mr. P. M. Yeung for providing technical help.

[1] R. R. Joyce, K. H. Hinkle, L. Wallace, M. Dulick, and D. L. Lambert, Astrophys. J. **116**, 2520 (1998).
[2] J. Jonsson, O. Launila, and B. Lindgren, Mon. Not. R. Astron. Soc. **258**, 49 (1992).
[3] K. H. Hinkle, D. L. Lambert, and R. F. Wing, Mon. Not. R. Astron. Soc. **238**, 1365 (1989).
[4] J. Jonsson, B. Lindgren, and A. G. Taklif, Astron. Astrophys. **246**, L67 (1991).
[5] J. F. Harrison, Chem. Rev. **100**, 679 (2000).
[6] Q. Ran, W. S. Tam, C. Ma, and A.S-C. Cheung, J. Mol. Spectrosc. **198**, 175 (1999).
[7] A.S-C. Cheung, Q. Ran, W. S. Tam, D. K-W. Mok, and P. M. Yeung, J. Mol. Spectrosc. **203**, 96 (2000).
[8] Q. Ran, W.S. Tam, and A.S-C. Cheung, Paper RA10, 55th Ohio State University International Symposium on Molecular Spectroscopy, Columbus, Ohio, June 2000.
[9] A.S-C. Cheung, J. Chin. Chem. Soc. (Taipei) **48**, 283 (2001).
[10] Q. Ran, W.S. Tam, A.S-C. Cheung, and A.J. Merer (to be published).
[11] Q. Shi, Q. Ran, W. S. Tam, J.W-H. Leung, and A.S-C. Cheung, Chem. Phys. Lett. **339**, 154 (2001).
[12] D. L. Lambert and R. E. S. Clegg, Mon. Not. R. Astron. Soc. **191**, 367 (1980).
[13] M. Marcano and R. F. Barrow, J. Phys. B **3**, L121 (1979).
[14] R. J. Winkel, Jr., S. P. Davis, and M. C. Abrams, Appl. Opt. **35**, 2874 (1996).
[15] N. Andersson, S. P. Davis, G. Edvinsson, and R. J. Winkel, Jr., Phys. Scr. **64**, 134 (2001).
[16] R. A. Frosch and H. M. Foley, Phys. Rev. **88**, 1337 (1952).
[17] C. H. Townes and A. L. Schawlow, *Microwave Spectroscopy* (Dover, New York, 1975).
[18] E. Hirota, *High Resolution Spectroscopy of Transient Molecules* (Springer, Berlin, 1985).
[19] B. Simard, S. A. Mitchell, M. R. Humphiers, and P. A. Hackett, J. Mol. Spectrosc. **129**, 186 (1988).
[20] S. Gerstenkorn, J. Verges, and J. Chevillard, *Atlas des Spectres d'Absorption de la Molecule d'iode, 11000-14000 cm*$^{-1}$ (Presses du CNRS, Paris, 1982).
[21] R. Basics, A. Bernard, and J. d'Incan, C. R. Seances Acad. Sci., Ser. B **276**, 272 (1971).
[22] R. Bascis and A. Bernard, Can. J. Phys. **51**, 648 (1973).
[23] M. Barnes, A. J. Merer, and G. F. Metha, J. Chem. Phys. **103**, 8360 (1995).
[24] A. G. Adam and J. R. D. Peers, J. Mol. Spectrosc. **181**, 24 (1997).
[25] See EPAPS Document No. E-JCPSA6-117-019232 for the observed line positions of the $B\,^2\Sigma^+$–$X\,^2\Sigma^+$ (0,0) band of LaS. This document may be retrieved via the EPAPS homepage (http://www.aip.org/pubservs/epaps.html) or from ftp.aip.org in the directory /epaps/. See the EPAPS homepage for more information.
[26] D. A. Fletcher, C. T. Scurlock, K. Y. Jung, and T. C. Steimle, J. Chem. Phys. **99**, 4288 (1993).
[27] T. D. Varberg, R. W. Field, and A. J Merer, J. Chem. Phys. **95**, 1563 (1991).
[28] I. M. Mills, T. Cvitas, K. Homann, and N. Kallay, *Quantities, Limits, and Symbols in Physical Chemistry* (Blackwell Scientific, Oxford, 1988).
[29] J. R. Morton, K. F. Preston, J. Magn. Reson. (1969-1992) **30**, 577 (1978).
[30] L. B. Knight, Jr., A. Ligon, R. W. Woodward, D. Feller, and E. R. Davidson, J. Am. Chem. Soc. **l07**, 2857 (1985).
[31] T. Törring, K. Zimmermann, and J. Hoeft, Chem. Phys. Lett. **151**, 520 (1988).
[32] W. J. Childs, G. L. Goodman, L. S. Goodman, and L. Young, J. Mol. Spectrosc. **119**, 166 (1986).